Contribution from the Lash Miller Chemical Laboratories and Erindale College, Department of Chemistry, University of Toronto, Toronto, Ontario, M5S 1A1, Canada, and the General Electric Company Corporate Research and Development, Schenectady, New York 12301

SCF-Xα-SW Molecular Orbital Investigations of Binary Zerovalent Carbonyl Complexes of the Group 1B Elements. Comparison with Matrix-Isolation Experimental Studies

DOUGLAS F. McINTOSH,* GEOFFREY A. OZIN,* and RICHARD P. MESSMER

Received August 22, 1980

The binary carbonyl complexes of copper, silver, and gold represent a unique series of molecules in terms of their electronic and geometrical makeup, bonding properties, and carbonyl force constant trends. They can be generated by metal atom synthetic techniques at 10-12 K and have an independent existence only when trapped in cryogenic matrices such as Ne, Ar, Kr, Xe, CO, and N_2. Above 77 K they all decompose to CO and microcrystals of the respective metal. All of the known mononuclear complexes display intense visible absorptions which are responsible for their characteristic hues. The present study reports on detailed SCF-Xα-SW calculations for $M(CO)_n$ (where M = Cu, Ag, n = 1-3; M = Au, n = 1, 2) as well as for the interesting linkage isomer (OC)Au(OC), the possible existence of the latter having been speculated upon in the original Au atom-CO matrix system. The results of this study permit a satisfactory rationale for the thermal lability of the complexes in terms of dominant σ-bonding M-C interaction with some pπ-π*, yet minimal dπ-π*, charge transfer from the metal to the CO ligand(s). This proposal is reinforced by comparisons with the results of a similar set of SCF-Xα-SW calculations for the series $Ni(CO)_n$ (where n = 1-4). The computational results also satisfactorily account for the optical spectra of a number of the group 1B carbonyl complexes and provide a clearer picture of the differences in the electronic structures of gold dicarbonyl and its isocarbonyl isomer and, with it, a deeper appreciation of their vibrational and optical properties. Finally, a bonding scheme can be formulated which provides a coherent explanation of the so-called "anomalous" CO force contant trend observed for the binary group 1B carbonyls, vis-ă-vis the "normal" trend seen in, for example, the analogous group 8 binary carbonyls.

Introduction

The recent syntheses, by cryochemical methods, of the binary, zerovalent, carbon monoxide complexes of copper,[1] $Cu(CO)_n$ (n = 1-3), silver,[2] $Ag(CO)_n$ (n = 1-3), and gold,[3] $Au(CO)_n$ (n = 1, 2) have opened a new class of compounds of the group 1B elements to chemical and physical investigation. Concomitant with the report of the syntheses of these complexes came the recognition of a number of problems concerning their electronic and vibrational characteristics.

The variation of the primary CO stretching force constants with coordination number was noted in one of the original papers.[2] When plotted as a function of the coordination number, it can be seen that a "V"-shaped curve arises (see Figure 1). This is distinctly different from similar curves plotted for the binary carbonyls of the group 8 metals[4] (see Figure 2). In the latter case, one obtains monotonically increasing functions. So that this "anomalous" trend in the CO force constants of the group 1B carbonyls could be rationalized, certain assumptions were made concerning the involvement of the d orbitals of the respective metals in the overall bonding schemes. Indeed, the d orbitals were largely ignored and the bonding mechanism was centered on a simplified s/p hybridization scheme.[2] It became obvious, however, that what was needed was a more rigorous and accurate treatment of the electronic structure of these complexes in order to properly interpret the infrared and ultraviolet-visible data obtained at the time.

The original report of the binary carbonyls of gold[3] also included speculations concerning the existence of an isocarbonyl(carbonyl) isomer of $Au(CO)_2$. Information available at that time tended to favor the isocarbonyl(carbonyl) isomer over a perturbed form of $Au(CO)_2$ when the "dicarbonyl" was formed in solid carbon monoxide. Since this interpretation was based, in part, on ultraviolet-visible band assignments from extended Hückel molecular orbital calculations, it was clear that perhaps a reevaluation in terms of a more accurate method was in order.

Part of the infrared evidence for the isocarbonyl(carbonyl) isomer was based on infrared intensity calculations. To obtain a good fit of the experimental data, it was necessary to orient the local carbonyl dipoles as I and II. While it is not in-

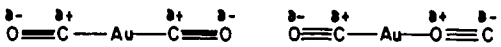

I II

conceivable to have a positive charge on an oxygen atom and a negative charge on a carbon atom, as in model II above, it does seem unlikely. The use of a model such as III would

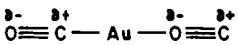

III

result in the relative inversion of the intensities of the bands ascribed to the isocarbonyl and carbonyl ligands, respectively. Thus, it became critically important to determine the relative charge distributions in these complexes.

Accordingly, SCF-Xα-SW molecular orbital calculations were performed on the entire series of binary, zerovalent, carbon monoxide complexes of the group 1B elements, including model calculations on the "normal" dicarbonyl of gold and its isocarbonyl(carbonyl) isomer. To help assess the extent of σ/π involvement of the metal and ligand orbitals in these complexes, similar calculations were performed on the $Ni(CO)_n$ (where n = 1-4) series. The result is a deeper appreciation of the basic electronic structures of all of these complexes, an excellent match between the predicted and observed excitation absorptions of a number of these complexes and a resolution of the gold dicarbonyl problem. Moreoever, the problem of the "anomalous" force constant trend could also be resolved.

* To whom correspondence should be addressed at the University of Toronto.

(1) H. Huber, E. P. Kündig, M. Moskovits, and G. A. Ozin, *J. Am. Chem. Soc.*, **97**, 2097 (1975).
(2) D. McIntosh and G. A. Ozin, *J. Am. Chem. Soc.*, **98**, 3167 (1976).
(3) D. McIntosh and G. A. Ozin, *Inorg. Chem.*, **16**, 51 (1977).
(4) E. P. Kündig, D. McIntosh, M. Moskovits, and G. A. Ozin, *J. Am. Chem. Soc.*, **95**, 7234 (1973).

0020-1669/81/1320-3640$01.25/0

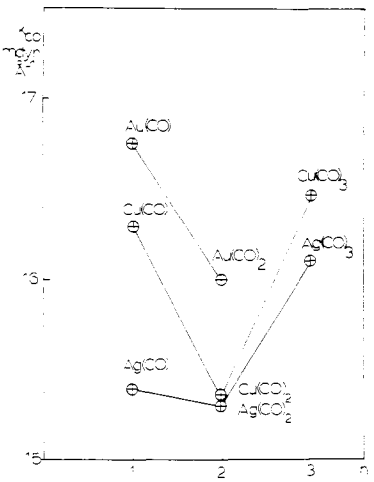

Figure 1. Graphical representation of the Cotton–Kraihanzel CO bond stretching force constants for $M(CO)_n$ (where M = Cu, Ag, n = 1–3; M = Au, n = 1, 2) as a function of n (taken from ref 2).

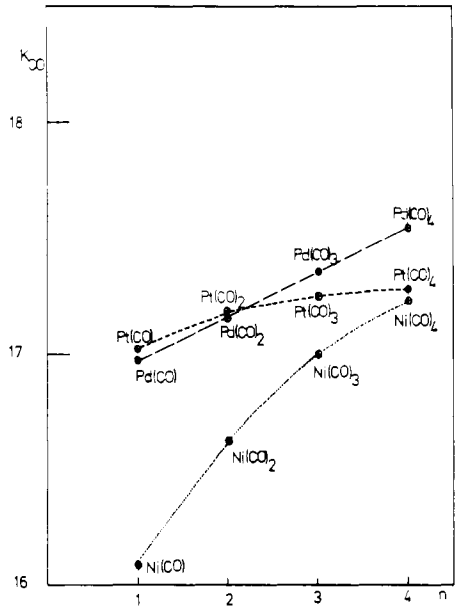

Figure 2. Graphical representation of the Cotton–Kraihanzel CO bond stretching force constants for $M(CO)_n$ (where M = Ni, Pd, Pt, n = 1–4) as a function of n (taken from ref 4).

Calculational Details

The electronic structure calculations were carried out within the framework of the self-consistent-field-Xα-scattered-wave method[5] by initially performing SCF-Xα atomic calculations using a computer program identical with that of Herman and Skillman,[6] except for the inclusion of a variable α parameter in the expression for the exchange-correlation term. α parameters for carbon, oxygen, copper, silver, and gold were taken from the tabulations of Schwarz.[7] A superposition of the charge densities derived from these numerically determined atomic orbitals was then used as the starting point for the molecular calculation. Boundary conditions (i.e., the values of the atomic sphere radii) were derived by using Norman's method.[8]

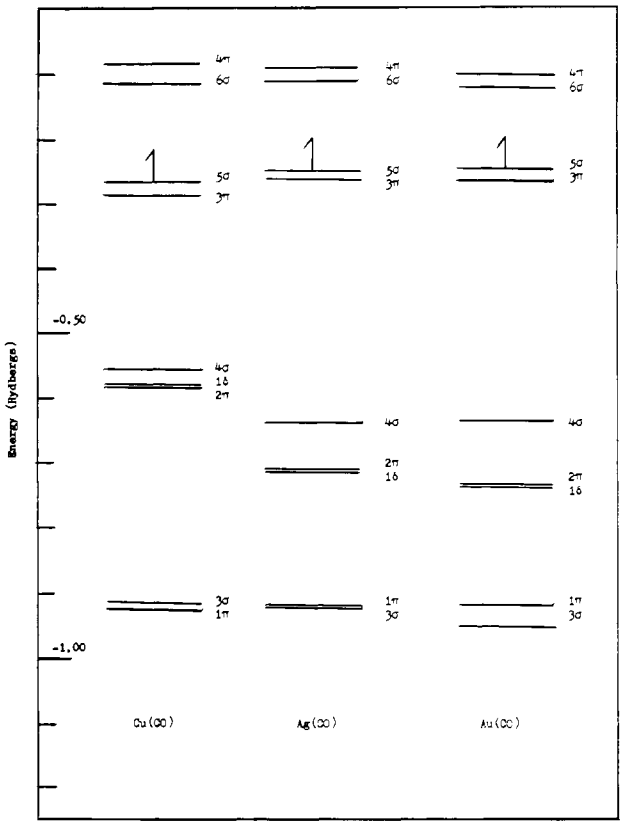

Figure 3. SCF-Xα-SW spin-restricted energy level schemes for Cu(CO), Ag(CO), and Au(CO). Energies are quoted in Rydberg units. The highest occupied molecular orbital is indicated by the position of the spin-up electron.

Partial wave expansions were included for values of L up to 4 for the outer sphere ("OUT"), 2 for the metal atoms, and 1 for the carbon and oxygen atoms. The α values for the outer sphere and the intersphere regions were set equal to the valence-electron weighted average of the α values of the constituent atoms. The complete structural parameters and partial wave analyses for the ground-state spin-restricted calculations of the monocarbonyls of copper, silver and gold, the dicarbonyls of copper and silver, the tricarbonyls of copper and silver, and the two linkage isomers of the dicarbonyl of gold are collected in Appendices I–IV, respectively, of the supplementary material.

The zerovalent carbonyl complexes of the three metals were assumed to adopt regular geometries. The mono- and dicarbonyls, with $C_{\infty v}$ and $D_{\infty h}$ symmetries, were oriented along the z axis. The tricarbonyls (D_{3h}) were placed in the xy plane with one of the vertical planes of symmetry as the xz plane. Except for the two linkage isomers of the dicarbonyl of gold, all metal–carbon bond distances were assumed to be equal to the sum of the single-bond "covalent" radii of the atoms (C 0.77, Cu 1.17, Ag 1.34, and Au 1.34 Å).[9] The C–O bond distance was assumed to be approximately 1.15 Å throughout.

Distances and coordinates, in the following discussions, are expressed as multiples of the Bohr radius of the hydrogen atom (0.529 177 06 (44) Å) and energies are given in terms of the

(5) (a) K. H. Johnson and F. C. Smith, Jr., *Phys. Rev. B: Solid State*, **5**, 831 (1972); (b) J. C. Slater and K. H. Johnson, *ibid.*, **5**, 844 (1972); (c) P. Weinberger and K. Schwarz, *Int. Rev. Sci.: Phys. Chem., Ser. Two*, **1**, 255 (1975); (d) K. H. Johnson, *Adv. Quantum Chem.*, **7**, 143 (1973); (e) N. Rösch, *NATO Adv. Study Inst. Ser., Ser. B*, **24**, 1 (1977); (f) J. W. D. Connolly, "Semiempirical Methods of Electronic Structure Calculation", G. A. Segal, Ed., Plenum Press, New York, 1977, Part A, p 105; (g) J. C. Slater, "The Calculation of Molecular Orbitals", Wiley, New York, 1979.

(6) F. Herman and S. Skillman, "Atomic Structure Calculations", Prentice-Hall, Englewood Cliffs, NJ, 1963.

(7) (a) K. Schwarz, *Phys. Rev. B: Solid State*, **5**, 2466 (1972); (b) *Theoret. Chim. Acta*, **34**, 225 (1974).

(8) (a) J. G. Norman, Jr., *J. Chem. Phys.*, **61**, 4630 (1974); (b) *Mol. Phys.*, **31**, 1191 (1976).

(9) Sargent-Welch Periodic Table S-18806, Sargent-Welch Scientific Company, Skokie, IL, 1968.

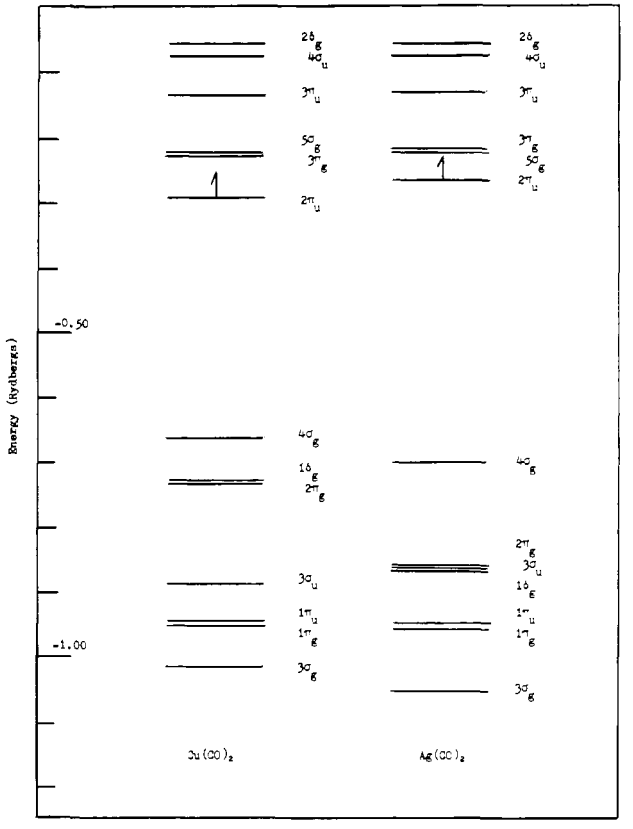

Figure 4. SCF-Xα-SW spin-restricted energy level schemes for $Cu(CO)_2$ and $Ag(CO)_2$. Energies are quoted in Rydberg units. The highest occupied molecular orbital is indicated by the position of the spin-up electron.

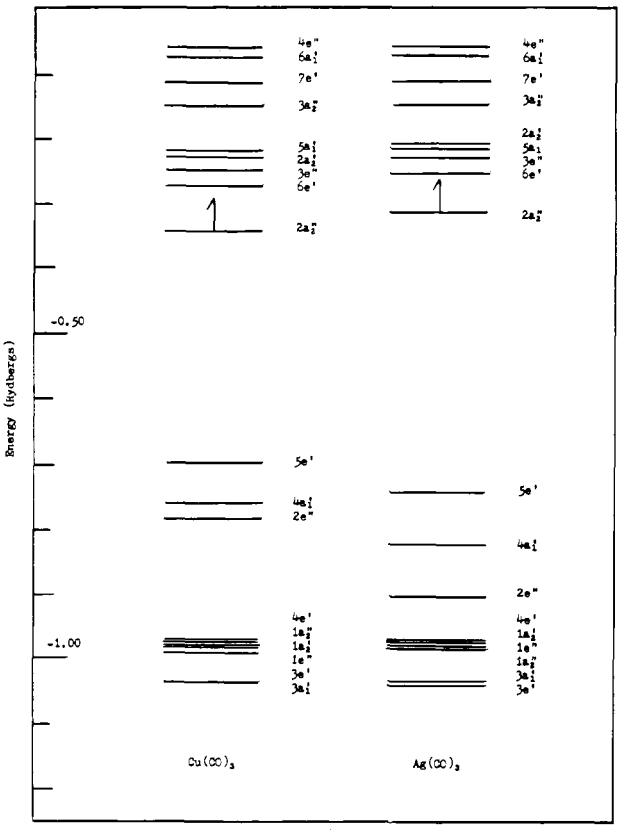

Figure 5. SCF-Xα-SW spin-restricted energy level schemes for $Cu(CO)_3$ and $Ag(CO)_3$. Energies are quoted in Rydberg units. The highest occupied molecular orbital is indicated by the position of the spin-up electron.

Rydberg unit (1.097 373 177 (83) × 10^5 cm^{-1}, 13.605 804 (36) eV).[10]

SCF-Xα-Scattered-Wave Calculations

The energy level diagrams for the spin restricted calculations of the monocarbonyls of copper, silver and gold, the dicarbonyls of copper and silver, and the tricarbonyls of copper and silver are depicted in Figures 3–5, respectively. Only in the case of the monocarbonyls was there any ambiguity in the choice of the ground-state electronic configuration where a near degeneracy of the 3π and 5σ levels occurred. Because of the implications of the ESR data,[1] however, the 5σ was chosen as the highest occupied molecular orbital. The three monocarbonyls were, therefore, described by the $^2\Sigma$ electronic term symbol in their ground-state configurations. Recent ab initio RHF-MO calculations[11] support this assignment for Cu(CO), and it seems likely that silver and gold monocarbonyl will also have the same electronic ground-state configuration.

The 5σ molecular orbital contour diagrams for Cu(CO) and Ag(CO) are illustrated in Figure 6 (the contour diagram for Au(CO) is virtually identical with that of Ag(CO) and has, thus, been omitted). The figure clearly shows that the lone unpaired electron resides in an orbital which is essentially metal s in character and has its spatial orientation directed away from the carbonyl ligand.

Examination of the partial wave analyses of Cu(CO) reveals some interesting points on the interaction of the constituent atomic orbitals. The lowest lying molecular level in the monocarbonyl, the 1σ, corresponds to the localized σ bond between the carbon and oxygen atoms, formed from the overlap of sp hybrid orbitals. The next highest level, the 2σ, can be crudely described as a lone pair of electrons situated on the oxygen atom. Significant interaction between the metal and carbon monoxide is not observed in molecular levels below the 3σ (the 1π orbital is best described as a pair of localized π bonds between the carbon and oxygen atoms, formed from the sideways overlap of p type atomic orbitals). The 3σ orbital can be regarded as being formed from the overlap of the 3σ level of the carbon monoxide molecule (the lone pair of electrons on the carbon atom) with an sp-type hybrid orbital on the copper atom. This eigenvector corresponds to the first partner of the pair of orbitals normally used to describe the synergic bonding mechanism in metal carbonyls.[12] The other partner, which would have accounted for the back transference of charge density from a metal d orbital to the π^* level of CO, is the 2π energy level. Examination of the partial wave analysis of Cu(CO) shows that this level is almost exclusively metal d in character. It is primarily the 3σ orbital which provides significant bonding interaction between the metal and the ligand.

The remainder of the nonbonding d orbitals of copper (1δ, 4σ) have energies similar to that of the 2π molecular level. Although both the 4σ and 5σ orbitals are essentially nonbonding levels, it could be argued that they display very slight tendencies toward weakly bonding and weakly antibonding interaction, respectively. This effect is more noticeable in the cases of Ag(CO) and Au(CO) where the d orbitals of silver and gold have dropped in energy, relative to those of copper, and the 4σ level is now separated from the other metal d orbitals by a larger energy difference. The distinctly larger mutual interaction of these two orbitals can be easily seen in Figure 3. There is also a greater contribution of the carbon monoxide basis functions, relative to those of the metal, to the

(10) E. R. Cohen and B. N. Taylor, *J. Phys. Chem. Ref. Data*, **2**, 663 (1973).
(11) H. Itoh and A. B. Kunz, *Z. Naturforsch., A*, **34A**, 114 (1979).
(12) F. A. Cotton and G. Wilkinson, "Advanced Inorganic Chemistry", 3rd ed., Wiley, New York, 1976, pp 684–688.

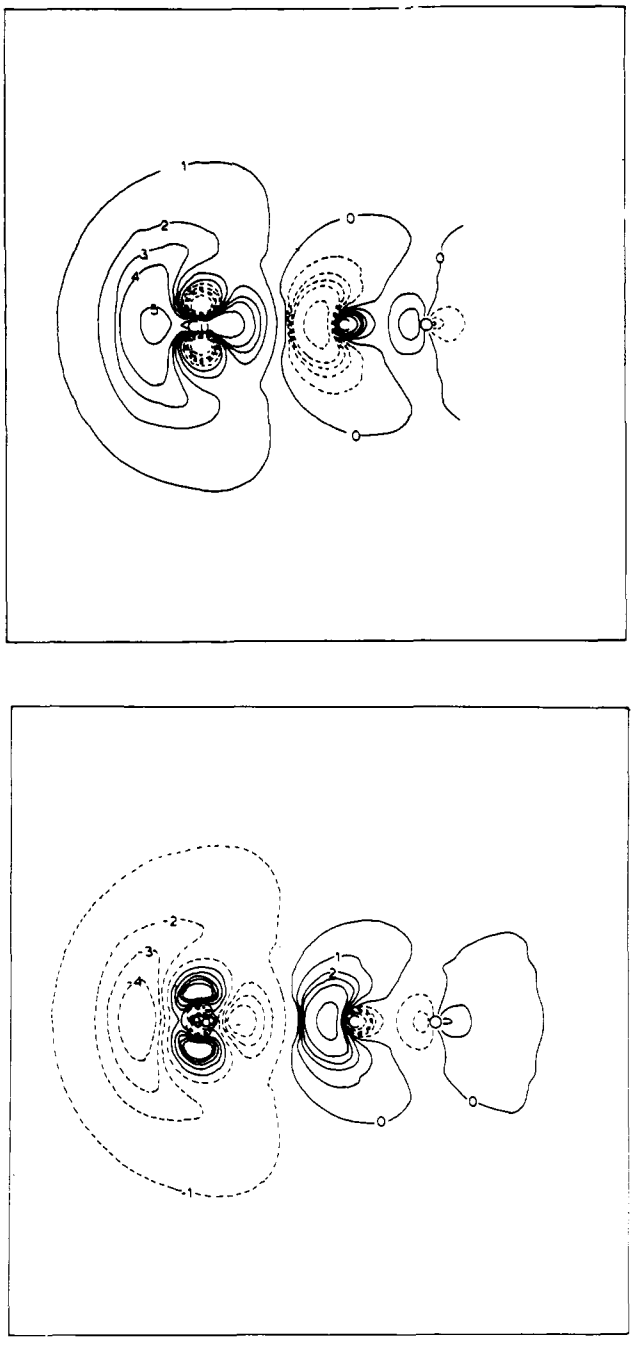

Figure 6. Wave function contour diagrams for the 5σ molecular orbitals of Cu(CO) and Ag(CO). Note that positive wave function contours are indicated by solid lines, whereas negative wave function contours are given by dashed lines. Contour specifications ((electrons/bohr^3)$^{1/2}$): 1, 0.03; 2, 0.06; 3, 0.08; 4, 0.10; 5, 0.15. The "0" contours represent nodal surfaces.

molecular orbitals in Ag(CO) and Au(CO) than there was in Cu(CO) (see the partial wave analyses in Appendix I). It must be remembered, though, that this effect is very small and that both the 4σ and 5σ orbitals have little net bonding (or antibonding) influence due to the greater polarizabilities of the silver and gold charge densities compared with that of copper.

As previously stated, the assignment of the ground-state electronic configurations presented no difficulty for the di- and tricarbonyls of copper and silver. In the former case, both $Cu(CO)_2$ and $Ag(CO)_2$ could be unambiguously described by a $^2\Pi_u$ electronic ground-state term symbol whereas, in the latter case, $Cu(CO)_3$ and $Ag(CO)_3$ were uniquely assigned a $^2A_2''$ electronic configuration. Without recourse to a full analysis, it can be determined from the partial wave analyses for the di- and tri-carbonyls (Appendices II and III, respectively) that, as was the case for the monocarbonyls, there is very little effective $d\pi-\pi^*$ back-bonding occurring in any of the other binary carbon monoxide complexes of copper and silver. Once again, major bonding interactions arise from the σ donation of charge density from the 3σ orbital of the CO ligands to the respective metals. In the dicarbonyls, the molecular orbitals showing significant metal–carbon σ interactions are the $3\sigma_g$ and the $3\sigma_u$ whereas these effects are restricted to the $3a_1'$, $3e'$ and, to a much lesser extent, the $4e'$ molecular orbitals in the tricarbonyls. Again, because of the slightly more diffuse nature of the silver atomic orbitals (and hence the greater polarizability of the atomic silver charge density), the mutual involvement of silver and carbon monoxide basis functions appears to be marginally greater in the intermediate molecular energy levels of $Ag(CO)_2$ and $Ag(CO)_3$. It must be emphasized again, though, that little net bonding (or antibonding) interaction will be achieved from these orbitals. The calculations indicate that the valence d orbitals of the group 1B metals act very much like closed-shell corelike energy levels.

Although there is little $d\pi-\pi^*$ bonding in the di- and tricarbonyls, there is an important molecular π level in each, namely, the $2\pi_u$ and the $2a_2''$, respectively. The contour diagrams for these orbitals are illustrated in Figure 7 and 8. Figure 7 shows the large π bond extended over the metal and carbon atoms, with charge density concentrated on the ligands. Of considerable significance is the observation that it is *only* the metal p orbital which participates in the metal–ligand interaction in this orbital. The same is true of the $2a_2''$ molecular orbital of the tricarbonyls, although the contour diagrams in Figure 8 have a deceptive appearance. This is due to the fact that the *xz* plane of the tricarbonyl is plotted in this figure and the other two carbonyl ligands, being situated above and below the plane, show no contour contributions in *this* plane. One could, of course, plot the two planes which encompass the metal atom and the other two carbonyl ligands, although they would be identical with the one illustrated in Figure 8. When placed together, however, the three plots would give an accurate pictorial representation of the $2a_2''$ orbital.

Because of the recent controversy raised by Larsson and Braga[13] and Bursten, Freier, and Fenske[14] over the possible misinterpretation of the importance of $d\pi-\pi^*$ back-bonding in $Cr(CO)_6$ by Johnson and Klemperer[15] and in $Ni(CO)_4$ by Johnson and Wahlgren[16] it was thought that a comparison between the group 1B metal carbonyls and a set of carbonyls which might be expected to exhibit considerable $d\pi-\pi^*$ back-bonding would be appropriate. Without the benefit of the LCAO projection method of Bursten and Fenske,[17] it would be difficult to make definite assessments of the amount of σ and π charge populations for the important orbitals of the group 1B metal carbonyls. However, it is possible to compare the muffin-tin results of the two metal–carbonyl systems among themselves and relate them to the findings of Bursten, Freier, and Fenske[14] for a known system. Accordingly, SCF–Xα–SW calculations were performed on $Ni(CO)_n$, where n = 1–4, with exactly the same procedures as in the case of the group 1B metal carbonyls. Geometries for the mono-, di-, and tricarbonyls of nickel were identical with those of the similar copper series except for the assumption of a metal

(13) S. Larsson and M. Braga, *Int. J. Quant. Chem.*, **15**, 1 (1979).
(14) B. E. Bursten, D. G. Freier, and R. F. Fenske, *Inorg. Chem.*, **19**, 1810 (1980).
(15) J. B. Johnson and W. G. Klemperer, *J. Am. Chem. Soc.*, **99**, 7132 (1977).
(16) K. H. Johnson and U. Wahlgren, *Int. J. Quant. Chem., Symp.*, **6**, 243 (1972).
(17) B. E. Bursten and R. F. Fenske, *J. Chem. Phys.*, **67**, 3138 (1977).

Table I. The $d\pi$–π^* Orbitals (%) of $M(CO)_n$ (M = Ni, Cu; n = 1-3)

species	E^a	Ni	C	O	inter-sphere	E^a	Cu	C	O	inter-sphere
M(CO) 2π	-0.4476	82.39 (99.86% d)	2.81	3.27	10.91	-0.5851	92.69 (99.98% d)	0.50	1.37	5.00
$M(CO)_2$ $2\pi_g$	-0.5117	84.66 (100% d)	1.23	1.73	9.38	-0.7324	92.81 (100% d)	0.04	1.25	4.59
$M(CO)_3$ $2e''$	-0.5788	88.46 (100% d)	0.33	0.78	8.18	-0.7830	93.00 (100% d)	0.004	0.74	4.75

[a] Energies are given in terms of the Rydberg unit.

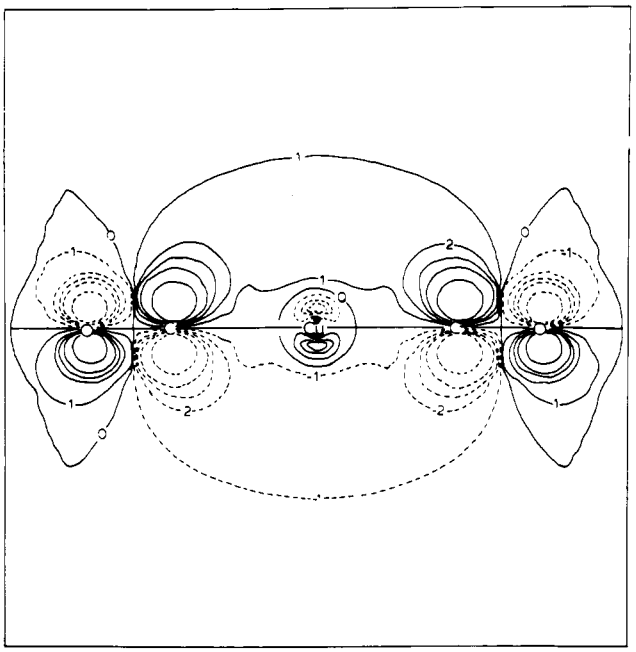

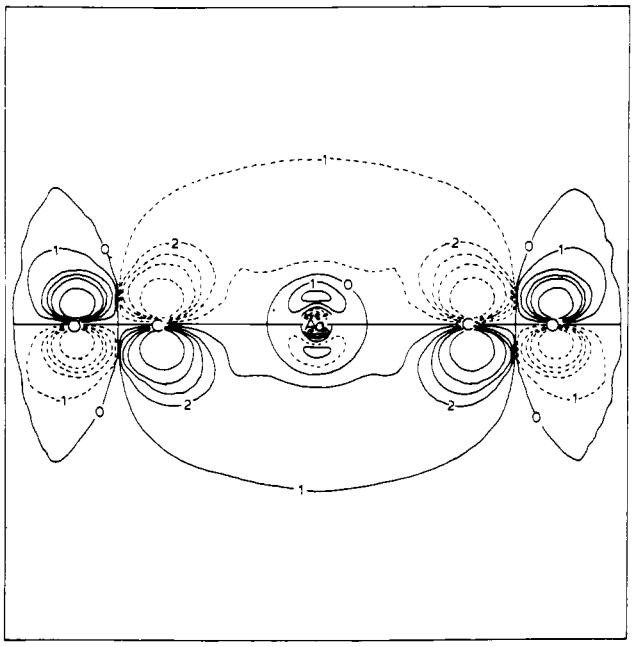

Figure 7. Wave function contour diagrams for the $2\pi_u$ molecular orbitals of $Cu(CO)_2$ and $Ag(CO)_2$. See Figure 6 for orbital and contour specifications.

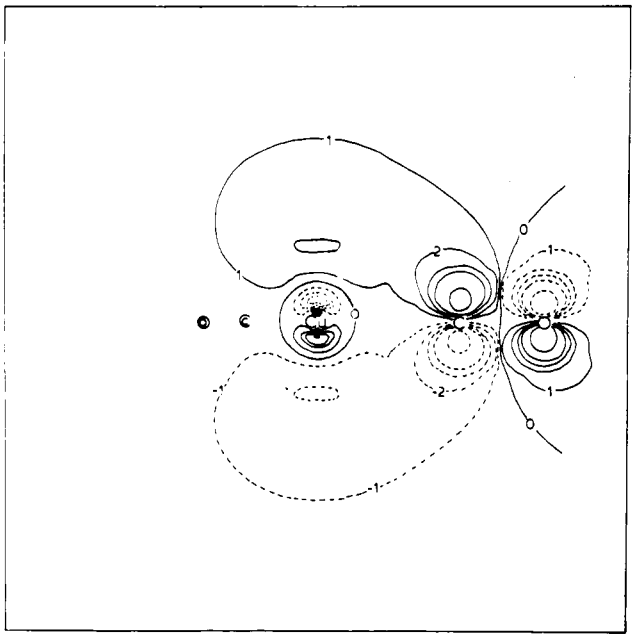

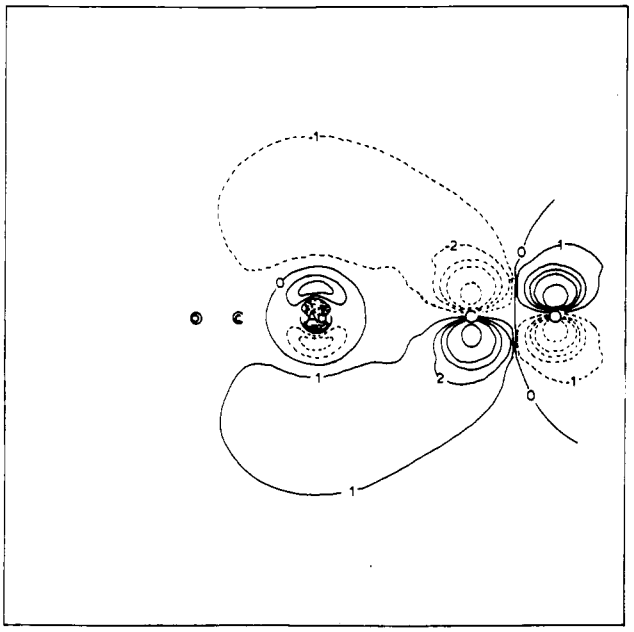

Figure 8. Wave function contour diagrams for the $2a_2''$ molecular orbitals of $Cu(CO)_3$ and $Ag(CO)_3$. See Figure 6 for orbital and contour specifications. Note that only the xz plane has been plotted in these figures.

covalent radius of 1.15 Å for nickel.[9]

A simplified tabulation of the charge densities of the mono-, di-, and tricarbonyls of nickel and copper for the major $d\pi$–π^* orbitals is presented in Table I. As Bursten, Freier, and Fenske point out, the lobes of the π^* orbital of carbon monoxide centered on the carbon atom are very diffuse.[14] Thus, one would expect that a significant portion of the charge density derived from the sideways overlap of a metal d orbital and the π^* orbital would be located in the intersphere region of space which, in the muffin-tin approximation, would be volume averaged throughout this region to a constant value. Thus, a relatively small increase in the amount of charge density located in the intersphere region might correspond to a substantially greater degree of $d\pi$–π^* bonding. As indicated in Table I, there is a considerable increase in the amount of charge density located in the intersphere region for all three

Table II. Partial Wave Analyses of the Major σ/π Orbitals of $Ni(CO)_4$

orbital	E^a	occupancy	outer	Ni	C	O	charge
$3a_1$	-1.0417	2.00	0.24	14.16	11.47	1.52	% charge
			47.48	100.00	67.83	96.12	% s
					32.17	3.88	% p
							% d
			37.21				% f
			15.30				% g
				33.66			% charge intersphere
2e	-0.6527	4.00	0.02	86.51	0.23	1.02	% charge
							% s
					100.00	100.00	% p
			37.49	100.00			% d
							% f
			62.51				% g
				8.49			% charge intersphere
$4t_2$	-0.9660	6.00	0.15	22.31	12.10	1.59	% charge
					48.39	0.47	% s
			25.92	15.26	51.61	99.53	% p
			51.61	84.74			% d
			19.46				% f
			3.01				% g
				22.79			% charge intersphere
$5t_2$	-0.5746	6.00	0.13	69.63	2.15	1.18	% charge
					45.42	2.33	% s
			62.68	3.62	54.58	97.67	% p
			8.98	96.38			% d
			13.39				% f
			14.95				% g
				16.93			% charge intersphere

[a] Energies are given in terms of the Rydberg unit.

carbonyls of nickel, compared with those of copper. Moreover, there is a significant increase in the amount of charge density in the carbon spheres with a concomitant decrease in the amount of charge in the metal sphere.

As a point of reference to the results of Bursten, Freier, and Fenske, an SCF–Xα–SW calculation was also performed on $Ni(CO)_4$. In the case of a tetrahedral molecule, the σ and π molecular charge densities no longer factor, as they did in the cases of the mono-, di-, and tricarbonyls, into in-plane and out-of-plane molecular orbitals because of the basic shape of the molecule but, rather, one obtains a mixing of the σ and π sets. From simple group theoretical considerations,[18] it may be shown that the σ orbitals have a_1 and t_2 symmetries while the π orbitals have e, t_1, and t_2 symmetries. Of the latter set, there are no s, p, or d orbitals on the metal which have t_1 symmetry. The partial wave analyses of the molecular orbitals of $Ni(CO)_4$ which have significant metal–carbon σ/π interactions are presented in Table II. From this tabulation it would appear reasonable to assign the major σ interactions to the $3a_1$ and $4t_2$ orbitals and the major π interactions to the 2e and $5t_2$ orbitals. It is interesting to note that whereas the percentage metal contribution in the $d\pi$-π^* orbitals of the mono-, di-, and tricarbonyls of nickel has ranged from about 82% to 88% (with the intersphere contribution in the range 11–8%, respectively), in the $5t_2$ orbital of the tetracarbonyl it has dropped to about 70% (with a concomitant increase in the intersphere contribution to 17%). The other π-type orbital of $Ni(CO)_4$, the 2e, is very similar to those of the mono-, di-, and tricarbonyls in that its metal contribution is about 86% (with an 8% intersphere contribution).

It was for $Ni(CO)_4$ that Bursten, Freier, and Fenske calculated a total of 1.11 electrons back-donated from the Ni 3d orbitals to the CO π^* orbitals. They concluded that this back-donation of 0.3 e/CO represented strong π back-bonding. (It is interesting to note that, even in the nickel carbonyl series, there appears to be a major increase in the amount of σ/π interaction on passing from the tri- to the tetracarbonyl.) With these results in mind, it is possible to reconsider the likelihood of strong π back-bonding in the cases of the copper carbonyls. By reference to Table I, it can be seen that the amount of intersphere charge density is generally about 0.3 times that of $Ni(CO)_4$ while the metal contributes about 93% to the overall orbital charge distribution compared with about 70% in the case of nickel (about 33% greater). In light of this comparison, it seems reasonable to reiterate that the amount of $d\pi$–π^* back-bonding in the group 1B metal carbonyls is minimal. Even though this will have to be confirmed by an LCAO projection, the above comparison tends to favor this view.

What is much less certain, though, is the degree of π back-bonding afforded by the highest occupied molecular orbitals of the di- and tricarbonyls, the $2\pi_u$ and the $2a_2''$. Since they are only singly occupied and are formed from the diffuse, high-energy p orbitals of the respective metals, it seems likely that these orbitals will not be able to significantly increase the bond order of the metal–carbon bond. These effects are somewhat offset, though, by the observation that most, if not all, of the charge density derived from the unpaired electron has been transferred to the ligands (see Figures 7 and 8). Since none of these carbonyls has been isolated by normal laboratory preparative methods, it is reasonable to expect that these π bonds are not very strong. It is important, however, to note that there is a discontinuous jump in the degree of π back-bonding on passing from the monocarbonyl to the dicarbonyl where, in the former, there was no possibility of π back-bonding except for the $d\pi$-π^* orbital. In the cases of the di- and tricarbonyls, there are the additional π back-bonding contributions afforded by the presence of the two, singly occupied molecular levels, the $2\pi_u$ and the $2a_2''$.

Comparison with Experiment

When $Cu(CO)_3$ and $Ag(CO)_3$ were synthesized by the co-condensation reactions of copper and silver atoms, respectively, with undiluted carbon monoxide gas at 10–12 K, the ultraviolet–visible spectra shown in Figure 9 were obtained. Molecular spectra (free of copper and silver atoms) characterized

(18) F. A. Cotton, "Chemical Applications of Group Theory", 2nd ed., Wiley, New York, 1971, pp 199–213.

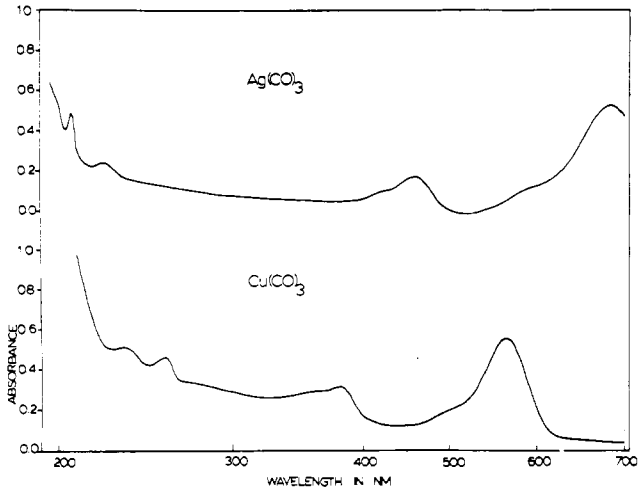

Figure 9. Ultraviolet–visible spectra of (A) $Ag(CO)_3$ and (B) $Cu(CO)_3$ in pure CO at 10–12 K.

Chart I. Absorbances (nm)

$Cu(CO)_3$	$Ag(CO)_3$
562 (s)	679 (s)
495 (w sh)	580 (w sh)
375 (ms)	457 (ms)
344 (w sh)	420 (w sh)
262 (w)	225 (w)
242 (w)	208 (w)

by two very intense, broad absorptions were obtained.[1,2]

It is of considerable interest to compare the optical spectra of $Ag(CO)_3$ and $Cu(CO)_3$, in Figure 9 and Chart I, with those predicted by the SCF–Xα–SW calculations.

The two broad visible absorptions, with their weak shoulders, of $Ag(CO)_3$ are shifted to lower energies compared with the corresponding absorptions of $Cu(CO)_3$. Examination of Figure 5 reveals that the only electronic excitations likely to produce absorptions centered in the visible region are those involving the excitation of the unpaired electron from the $2a_2''$ level to higher energy levels. While there appears to be a multitude of possible transitions to choose from, only transitions to the a_1' and e'' energy levels are spin and dipole allowed. Thus, one is obliged to assign the visible optical absorptions to electronic transitions from the $2a_2''$ molecular orbital to the 3e'', the $5a_1'$, the $6a_1'$, and finally the 4e'' energy levels. Likewise, in the case of the two weak ultraviolet absorptions, the only spin- and dipole-allowed transitions expected to be of reasonable intensity involve excitations of electrons from the $4a_1'$ and 2e'' orbitals to the $2a_2''$ orbital.

Transition-state calculations were not performed for either of the two tricarbonyls. It is possible, however, to obtain a crude estimate of the theoretically predicted excitation energies by simply taking the differences between the ground-state eigenvalues and comparing them with the experimentally observed energies. These results are given in Table III.

It is interesting to note that the SCF–Xα–SW calculations predict two pairs of visible absorptions for each complex, reminiscent of the two broad visible absorptions and their shoulders observed experimentally. Moreover, both the red and blue shifts of the visible and ultraviolet absorptions, respectively, observed on passing from copper to silver are reproduced by the calculations. While the calculated excitation energies under- or overestimate the observed energies, it must be remembered that only the ground-state energy differences were taken. Both spin-restricted and spin-unrestricted transition-state calculations (not to mention changes in the assumed geometries) would be expected to yield theoretical results more

Table III. Observed and Calculated Excitation Energies (cm^{-1}) for $Cu(CO)_3$ and $Ag(CO)_3$

obsd	calcd	assignt
	$Cu(CO)_3$	
17 800	10 400	$2a_2'' \rightarrow 3e''$
20 200	13 600	$2a_2'' \rightarrow 5a_1'$
26 700	29 300	$2a_2'' \rightarrow 6a_1'$
29 100	31 000	$2a_2'' \rightarrow 4e''$
38 200	45 600	$4a_1' \rightarrow 2a_2''$
41 300	48 600	$2e'' \rightarrow 2a_2''$
	$Ag(CO)_3$	
14 700	9 000	$2a_2'' \rightarrow 3e''$
17 200	10 900	$2a_2'' \rightarrow 5a_1'$
21 900	26 400	$2a_2'' \rightarrow 6a_1'$
23 800	27 600	$2a_2'' \rightarrow 4e''$
44 400	56 200	$4a_1' \rightarrow 2a_2''$
48 100	65 100	$2e'' \rightarrow 2a_2''$

in line with those observed. Even so, with this crude approximation of the energy differences, the calculated values are all generally within a factor of 2 of the observed quantities. The fact that the SCF–Xα–SW calculations predicted that only four visible transitions should be observed and that they would be grouped as two pairs of closely associated energy bands is impressive when viewed in light of the observed optical spectra of the neutral complexes.

The Gold Dicarbonyl Problem

So that a better understanding of the basic electronic structures of the two dicarbonyl isomers of gold could be obtained, SCF–Xα–SW calculations were performed on (OC)Au(CO) and (OC)Au(OC). The complete structural parameters and partial wave analyses for the ground-state spin-restricted calculations of these two molecules are collected in Appendix IV of the supplementary material.

The energy level diagrams for the spin-restricted calculations are illustrated in Figure 10. It is interesting to note that whereas the "normal" dicarbonyl has a ground state unambiguously determined by the calculations, namely, $^2\Pi_u$, a similar situation occurs for the isocarbonyl(carbonyl)gold isomer as did for the monocarbonyl complexes of copper, silver, and gold. In all of these molecules, the assignment of the ground-state electronic configuration is not clear since a choice must be made for the highest occupied molecular orbital between a σ and a π level. The similarity between the isocarbonyl(carbonyl)complex and gold monocarbonyl is actually much closer than might have been anticipated. Because of the poorer σ-donation and π-acceptance capabilities of a carbonyl ligand with its oxygen end oriented toward the metal, the isocarbonyl(carbonyl) complex behaves, electronically, very much like a monocarbonyl complex. The similarity between the energy level diagrams of (carbonyl) gold (Figure 3) and isocarbonyl(carbonyl)gold (Figure 10) is rather striking. Apart from the additional levels expected from the presence of a second carbonyl group (and minor bonding interactions), the two figures are virtually identical. This might suggest a relative instability of (OC)Au(OC) compared with (OC)Au(CO) since little net bonding energy is gained from the presence of the isocarbonyl ligand.

For the sake of conformity to the (OC)Au(CO) calculation, the 4π level was chosen as the highest occupied molecular orbital for (OC)Au(OC), although little difference would have resulted had the 8σ level been chosen (this was confirmed by actually performing a second "ground-state" calculation). Thus, both isomers were assigned π-type electronic ground-state configurations ($^2\Pi_u$ in the former case and $^2\Pi$ in the latter case).

As in the case of the dicarbonyls of copper and silver, gold dicarbonyl exhibits π delocalization of the odd electron through

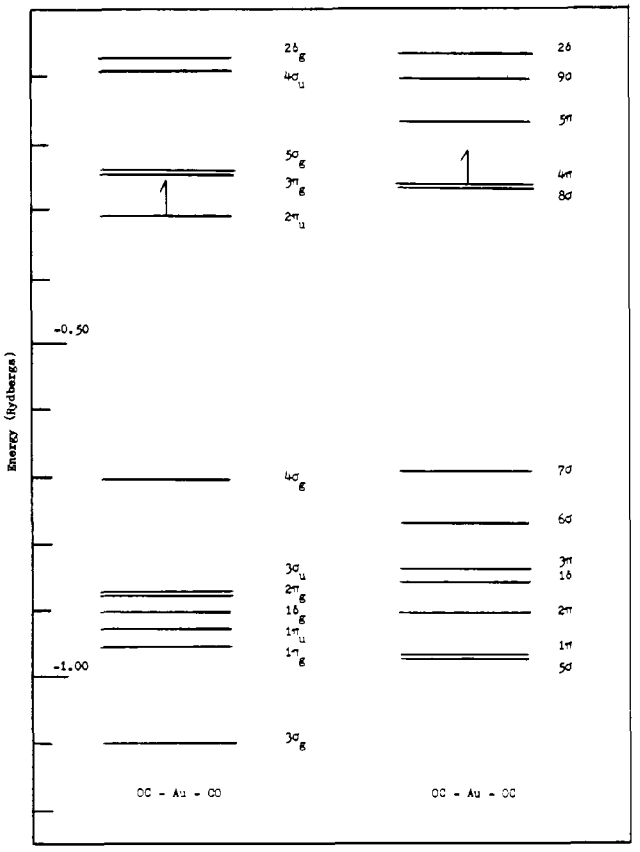

Figure 10. SCF–Xα–SW spin-restricted energy level schemes for (OC)Au(CO) and (OC)Au(OC). Energies are quoted in Rydberg units. The highest occupied molecular orbital is indicated by the position of the spin-up electron.

Table IV. Charge Distributions in the Binary Carbonyls of the Group 1B Metals

complex	metal	carbon	oxygen
Cu(CO)	-0.90	+0.96	-0.06
$Cu(CO)_2$	-0.74	+0.65	-0.28
$Cu(CO)_3$	-0.84	+0.58	-0.30
Ag(CO)	-0.71	+0.84	-0.13
$Ag(CO)_2$	-0.54	+0.58	-0.31
$Ag(CO)_3$	-0.61	+0.53	-0.32
Au(CO)	-0.64	+0.83	-0.19
$Au(CO)_2$	-0.92	+0.77	-0.31
$(O_1C_1)Au(OC)$	-0.81	+0.77 (C), +0.73 (C_1)	-0.36 (O), -0.34 (O_1)

the exclusive participation of the gold p orbital with the π^* orbitals on the carbonyl ligands. This is seen to best advantage in the orbital contour diagram of the $2\pi_u$ level in Figure 11. In contrast with this is the orbital contour diagram of the 4π level of (OC)Au(OC) in the same figure. It is readily apparent that back-bonding from the metal to the ligands occurs over only half the molecule, specifically, the carbonyl ligand which is oriented with its carbon end toward the gold atom. The other carbon monoxide moiety displays essentially a localized π^* orbital with minimal bonding interaction with the gold atom.

As a check on the relative carbonyl dipole orientations, atomic charge distributions (Table IV) were determined for the two isomers of gold dicarbonyl (the results for the other group 1B metal carbonyls have been included in the table for comparative purposes). The calculations were performed according to Norman's method of estimating the atomic charges.[19] This was accomplished by simply normalizing the

(19) J. G. Norman, Jr., *Inorg. Chem.*, **16**, 1328 (1977).

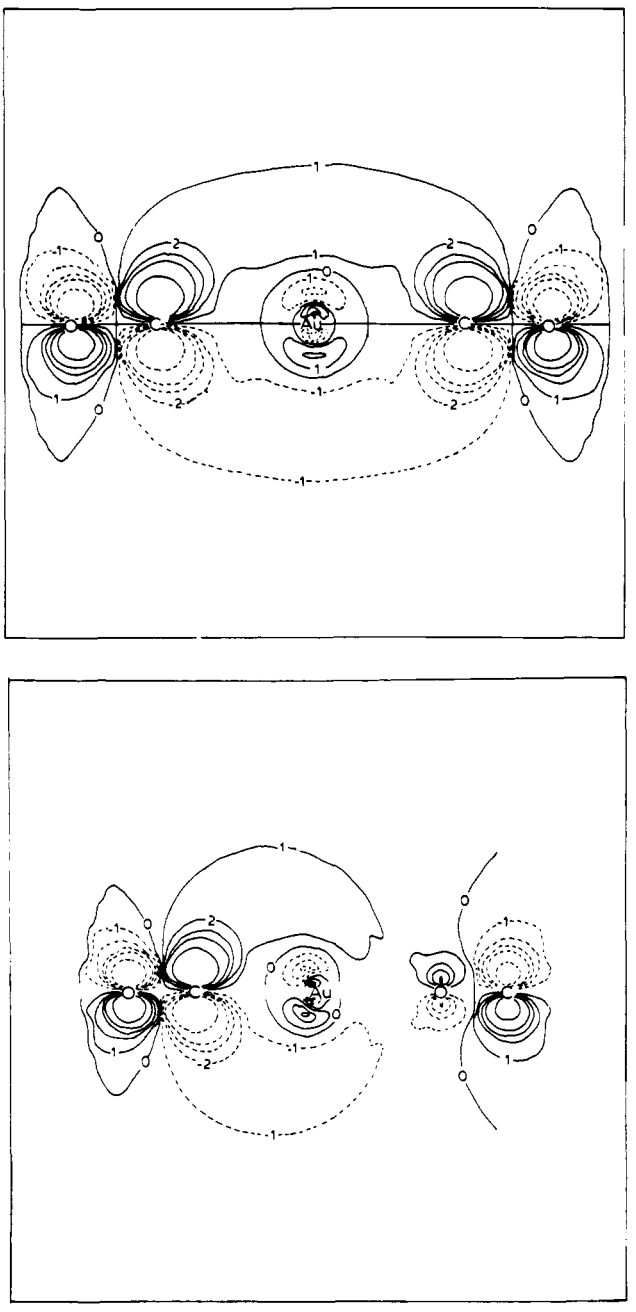

Figure 11. Wave function contour diagrams of the $2\pi_u$ and 4π molecular orbitals of (OC)Au(CO) and (OC)Au(OC), respectively. See Figure 6 for orbital and contour specifications.

total number of *valence* electrons within all the atomic spheres to the total number for the molecule and amounted to the partitioning of the intersphere and extramolecular charge among the atoms with use of weights equal to the number of valence electrons within each atomic sphere. While this is clearly a very approximate method of determining the atomic charges, and probably overestimates the charge separations, it should give a fair idea of the relative charges on the atoms.

It is significant that the calculations always placed a positive charge on the carbon atom and a negative charge on the oxygen atom. Thus, the assumptions made concerning the relative orientations of the local carbonyl dipoles in the intensity calculations[3] appear to be borne out by the molecular orbital calculations. Moreover, on the basis of these relative charge separations and the resulting dipole orientations of the carbonyl moieties, it would appear that the (OC)Au(CO) isomer of gold dicarbonyl is a preferable model, when examined in light of the intensity calculations. Assuming that one

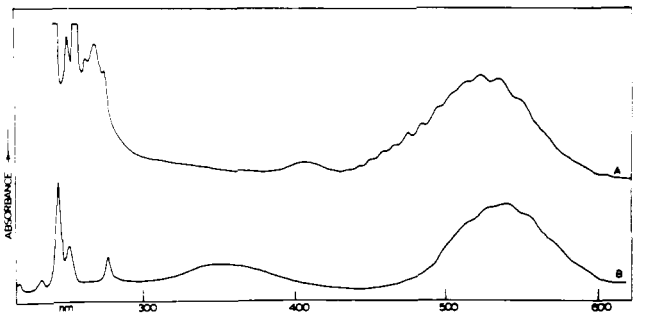

Figure 12. Ultraviolet–visible spectra of the products of the cocondensation reaction of gold atoms with (A) a mixed CO/Ar gas mixture 1/5 and (B) pure carbon monoxide at 10–12 K.

could transfer the relative orientations of the local carbonyl dipoles from these electronic structure calculations over to the infrared intensity determinations, one would expect an inversion of the relative intensities of the carbonyl and isocarbonyl stretching bands from that observed experimentally. Infrared intensity calculations based on the (OC)Au(CO) model match the experimentally observed values quite closely.[3]

Comparison of the ground-state energy level schemes for the two model complexes with the observed spectra also revealed some interesting differences between the two isomers. When gold atoms were cocondensed with a CO/Ar = 1/5 gas mixture the ultraviolet–visible spectrum displayed an intense absorption (with superimposed vibrational fine structure) in the visible region centered at roughly 520 nm together with a weaker absorption at about 407 nm (Figure 12). On cocondensing atomic gold with undiluted carbon monoxide, the two absorptions mentioned above red and blue shifted, respectively, to 538 and 350 nm. Futhermore, the intense visible band, centered at 538 nm in pure CO, showed distinct asymmetry probably due to a weaker absorption at similar energy, resulting in a shoulder on the major absorption band. This feature was not as noticeable in the case of the argon-diluted matrices because of the vibrational fine structure, although the presence of the weak shoulder could be discerned after a careful examination of the spectra.

Reference to the energy level diagram of (OC)Au(CO) (Figure 10) reveals that three spin- and dipole-allowed transitions can occur with energies centered in the visible region. All three transitions involve excitation of the unpaired electron from the $2\pi_u$ level to the $3\pi_g$, $5\sigma_g$, and the $2\delta_g$ levels, in order of increasing energy. Figure 10 clearly illustrates that the first two transitions mentioned above would be predicted to have nearly equal energies.

In the case of the (OC)Au(OC) isomer, however, the same figure shows that three visible absorptions would, again, be predicted and that they would also involve excitation of the unpaired electron from the 4π level to the 5π, 9σ, and 2δ levels. (It is interesting to note that had the 8σ level been chosen as the highest occupied molecular orbital then only two dipole-allowed transitions would have been predicted, namely, from this orbital to the 5π and the 9σ levels. The excitation to the 2δ level would have been a dipole-forbidden transition.)

Whereas the (OC)Au(CO) calculation indicates that two of the three transitions would have very nearly equal energies, the (OC)Au(OC) calculation predicts that the three transitions would have energies that were well separated. Thus, on the basis of the (OC)Au(OC) calculation, one might expect to see three well-resolved bands in the visible region (barring intensity considerations). Moreover, whereas the observed spectra indicate that the high- and low-energy visible bands blue and red shift, respectively, on passing from argon matrices to pure carbon monoxide, the model calculations predict that the absorptions should red and blue shift, respectively, on passing from (OC)Au(CO) to (OC)Au(OC).

Table V. Observed and Predicted Excitation Energies (cm^{-1}) for (OC)Au(CO) and (OC)Au(OC)

complex	transition	obsd	calcd
(OC)Au(CO)	$4\sigma_g \rightarrow 2\pi_u$	40 000	47 500
	$2\pi_u \rightarrow 2\delta_g$	24 600	27 400
	$2\pi_u \rightarrow 3\pi_g$	19 200	7 000
(OC)Au(OC)	$7\sigma \rightarrow 4\pi$	42 000	51 200
	$4\pi \rightarrow 2\delta$	28 600	23 000
	$4\pi \rightarrow 5\pi$	18 600	10 700

The observed optical energies are collected in Table V along with the calculated transition-state energies (in spin-restricted format). The only other spin- and dipole-allowed transition that might possibly be within the range of the experimental sampling techniques involves the excitation of an electron from a lower lying σ-type orbital to the highest occupied π-type level. Accordingly, the computed transition-state energies for the $4\sigma_g$ to $2\pi_u$ excitation energy in (OC)Au(CO) and the 7σ to 4π excitation energy in (OC)Au(OC) have also been included in Table V. Both absorptions clearly would be centered in the ultraviolet region. As such, only a crude estimate of the energy of the observed bands could be made due to the limits imposed by the spectrophotometer and the fact that atomic gold absorptions are also centered in that region and tend to overlap and obscure the molecular absorptions.

With all of the observed and calculated energy trends taken into consideration, it would appear that the (OC)Au(CO) model provides a better description of the behavior of the optical bands in both CO/Ar and pure CO matrices. The fact that the predicted energies are not closer to the observed energies could be a reflection of the degree of interaction of the respective matrices with the dicarbonyl molecule. Certainly, the shifts in the two (or three) absorptions cannot be properly accounted for by inverting one of the carbonyl ligands nor is the presence of the weak shoulder on the low-energy visible band correctly explained by the isocarbonyl(carbonyl) model. Within the restrictions imposed by the supposition of a given geometry, however, the gross features of the optical spectra can be accounted for by the (OC)Au(CO) molecule. The exact assignment of the intense band and its shoulder to the $2\pi_u$ to $5\sigma_g$ and $2\pi_u$ to $3\pi_g$ transitions, or vice versa, will have to await further transition-state and intensity calculations. (If the intense band turns out to be described as an excitation of the $2\pi_u$ electron to the $5\sigma_g$ molecular level, as it seems most likely to be, then the absorption might be crudely described as a charge-transfer type of transition originating from a mainly ligand-based orbital to one which is predominantly composed of metal basis functions (see the partial wave analysis for $Au(CO)_2$ in Appendix IV of the supplementary material). This would be consistent with the intense nature of the band.)

It might, as well, be informative to carry out a series of calculations involving the dicarbonyl with Ar, Kr, Xe, CO, and N_2 in the third site to determine the influence of a neighboring molecule on the relative spacings of the energy levels of (OC)Au(CO). A geometrical arrangement such as IV would

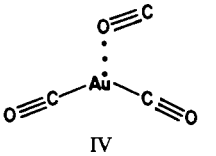

IV

certainly produce the observed inequivalence of the carbonyl ligands and, with the neighboring carbon monoxide ligand oriented with its oxygen end nearest the metal, would maintain the relative integrity of the dicarbonyl complex (cf. the calculation of (OC)Au(OC) with that of (OC)Au). Previous

studies of mixed CO/N_2 complexes of transition metals[20,21] have shown that the σ-donation and π-acceptance characteristics of N_2 are much poorer, on both counts, than CO. Thus, it might not be expected that dinitrogen could induce the formation of a mixed carbon monoxide/dinitrogen complex of the form $Au(CO)_2(N_2)$. It might be anticipated, however, that a geometrical arrangement of the dicarbonyl in solid dinitrogen matrices, with C_s substitutional site symmetry, should also result in a similar perturbation of the complex. Similarly, the placement of a noble-gas atom in the third site would also be expected to yield a perturbation of the electronic spectrum of the dicarbonyl without resulting in the inequivalence of the two carbonyl ligands. It would be interesting to investigate the ultraviolet–visible spectrum of the dicarbonyl complex in a series of mixed-CO/gas matrices to see whether the visible absorptions noted earlier are sensitive to the matrix environment. If so, then the concept of an isocarbonyl(carbonyl) complex could be safely dispelled. Such a study, coupled with theoretical investigations, might shed some additional light on the mode of interaction of the host molecules with the dicarbonyl complex.

The Anomalous Force Constant Trend

The problem of the discrepancy between the force constant trends of the group 8 and group 1B metal carbonyls, mentioned in the Introduction, can now be resolved with the aid of the SCF–Xα–SW results. A simplified bonding mechanism has already been invoked to explain the trend of the force constants of the group 1B metal carbonyls.[2] The basic ideas of this bonding scheme will now be reiterated in conjunction with the theoretical findings of this paper.

If one assumes that the synergic bonding mechansim,[12] usually used to explain the bonding in metal carbonyls, is operative in the group 8 metal carbonyls then, with the assumption that σ-bonding effects are relatively constant throughout the series $M(CO)_n$ (n = 1–4), variations in the infrared frequencies and the primary stretching force constants of the carbonyl ligands will be determined largely by changes in the π charge density and the relative back-donation of charge density from the metal to each of the ligands. If this is true, then, the greater the number of carbonyl ligands that compete for the same π charge density on the metal the larger will be the CO force constant since less charge density per carbonyl will be transferred to the π^* orbital of each ligand. One would thus expect to see a monotonically increasing function if the CO force constants were plotted with respect to the coordination number of the complexes for the full series $M(CO)_n$ (n = 1–4; M = Ni, Pd, Pt). This is indeed the case observed experimentally, as shown in Figure 2.

Since the Xα results indicate that the effectiveness of $d\pi$–π^* bonding is minimal for the group 1B metal carbonyls, one might adopt a simplified bonding scheme for these complexes which involves only s/p hybridization of the central metal atom. Such a scheme is illustrated in Figure 13 for the mono-, di-, and tricarbonyl complexes of copper, silver, and gold. Comparisons between these schematic figures and the highest occupied molecular orbitals of the three complexes (Figure 6–8) will indicate a remarkable similarity.

Under this simplified bonding scheme, it is readily apparent that the central metal atom adopts an sp-type hybridization in the cases of the mono- and dicarbonyls and sp^2 hybridization in the case of the tricarbonyl. What is unique, however, is the

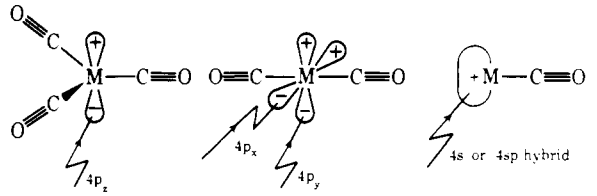

Figure 13. Pictorial representations of the hybridization schemes for the $M(CO)_3$, $M(CO)_2$, and M(CO) carbonyls of the group 1B metals.

location of the unpaired electron in each of the three complexes. In the monocarbonyl, the lone electron resides in one of the sp-hybrid orbitals on the metal whereas, in the di and tricarbonyls, the unpaired electron is located in an unhybridized p orbital on the metal. In the case of the monocarbonyl, then, it is impossible for the charge density resulting from the presence of the lone electron to be back-donated to the π^* orbital of the ligand since it is located in the σ framework of the complex. The opposite is true in the cases of the di- and tricarbonyls. There, the unpaired electron is directly involved in the π network of the complexes and may be equally shared by the ligands.

Accordingly, one would expect that, as was the case for the binary carbonyl complexes of the group 8 metals, the greater the number of ligands competing for the same charge density (in this case, one electron) the larger will be the CO stretching force constant. Figure 1 clearly shows an increase in the primary CO stretching force constant on passing from $M(CO)_2$ to $M(CO)_3$ (M = Cu, Ag). As expected, then, it is the monocarbonyl complex that is the "odd" molecule in the series. If one accepts the notion that the highest occupied orbital of the carbon monoxide molecule is weakly antibonding[12] and that ionization of CO, to form CO^+, is accompained by the removal of an electron from this orbital then one would expect to see a dramatic increase in the frequency of the molecule. This is indeed the case observed experimentally (ν(CO) = 2143, $\nu(CO^+)$ = 2184 cm^{-1}).[18] In a similar manner, it might be argued that with only the effects of σ donation from the ligand to the metal one would expect the primary CO stretching force constant of the monocarbonyl to be larger than that of the dicarbonyl. This is indeed observed experimentally (Figure 1). The fact that there is some $d\pi$–π^* charge transfer, especially in the monocarbonyl, is reflected by the fact that the force constant(s) and frequencies of the metal carbonyls are below that of free carbon monoxide.

Although this bonding mechanism is attractive because of its relative simplicity, it must be recognized that it basically ignores $d\pi$–π^* interactions completely. While these Xα calculations tend to support the notion that this type of bonding is minimal in the group 1B metal complexes, they do, nonetheless, indicate that there is some charge transferred from the metal d orbitals to the π^* orbitals of the ligands. However, they show that there should be a major increase in the amount of overall π bonding on passing from the monocarbonyls to the dicarbonyls. Thus, even if the LCAO projection were to indicate that $d\pi$–π^* interactions were *not* insignificant, it would still be reasonable to expect the observed trend in primary CO force constants. The s/p hybridization scheme may, therefore, be taken as an extreme simplification of the results of the Xα calculations. The complete confirmation of this model, though, will have to wait a detailed geometry optimization study.

Conclusions

The results of this study indicate that the binary carbon monoxide complexes of the group 1B elements should be thermally less stable than their counterparts of the group 8 elements due to the poorer π-bonding abilities of the metal d orbitals. The calculations indicate that the valence d orbitals on the metal centers behave more like closed-shell, corelike

(20) E. P. Kundig, M. Moskovits, and G. A. Ozin, *Can. J. Chem.*, **51**, 2737 (1973).
(21) M. Moskovits and G. A. Ozin in "Cryochemistry", M. Moskovits and G. A. Ozin, Ed., Wiley, New York, 1976, Chapter 8.
(22) G. Herzberg, "Molecular Spectra and Molecular Structure. I. Spectra of Diatomic Molecules", Van Nostrand, Princeton, NJ, 1950.

levels and have minimal participation in overall π-bonding schemes.

The fact that the Xα calculations provided such a close match between the observed and calculated optical trends for the tricarbonyls of copper and silver, that they provided a clear picture of the differences in the electronic structures of gold dicarbonyl and its isocarbonyl isomer (thereby giving a more reasonable interpretation of the infrared and ultraviolet–visible spectra than previously possible), and that they helped to yield a simplified view of the bonding schemes in these complexes, in which the "anomalous" force constant trend observed experimentally could be rationalized, all attest to the usefulness and accuracy of the SCF–Xα–SW method as a predictive tool.

Acknowledgment. The financial assistance of the Natural Sciences and Engineering Research Council of Canada's Operating, New Ideas, and Strategic Energy programs is greatly appreciated. In addition, the generous support of Imperial Oil of Canada, Erindale College, and the Lash Miller Chemical Laboratories is gratefully acknowledged.

Registry No. Cu(CO), 55979-21-0; $Cu(CO)_2$, 55979-20-9; $Cu(CO)_3$, 55979-19-6; Ag(CO), 59751-30-3; $Ag(CO)_2$, 59751-29-0; $Ag(CO)_3$, 58832-57-8; Au(CO), 60594-88-9; $Au(CO)_2$, 60594-90-3; (OC)Au(OC), 60582-72-1; Ni(CO), 33637-76-2; $Ni(CO)_2$, 33637-77-3; $Ni(CO)_3$, 26024-55-5; $Ni(CO)_4$, 13463-39-3.

Supplementary Material Available: Listings of partial wave analyses for spin-restricted SCF–Xα–SW calculations of M(CO) (M = Cu, Ag, Au) (Appendix I), of $M(CO)_2$ (M = Cu, Ag) (Appendix II), of $M(CO)_3$ (M = Cu, Ag) (Appendix III), and of (OC)Au(CO) and (OC)Au(OC) (Appendix IV) (52 pages). Ordering information is given on any current masthead page.

Contribution from the Departments of Chemistry, University of California, Irvine, California 92717, and Carnegie-Mellon University, Pittsburgh, Pennsylvania 15213

Molecular Orbital Theory of the Properties of Inorganic and Organometallic Compounds. 2. STO-*N*G Basis Sets for Fourth-Row Main-Group Elements

WILLIAM J. PIETRO,† EDWARD S. BLUROCK,† ROBERT F. HOUT, JR.,† WARREN J. HEHRE,*† DOUGLAS J. DEFREES,‡ and ROBERT F. STEWART‡

Received March 5, 1981

Extension of the STO-3G minimal basis set to the main-group fourth-row elements (Rb, Sr, In–Xe) has been proposed. Equilibrium geometries, calculated for a wide variety of simple molecules containing these elements, have been found to be in reasonable accord with the available experimental structural data.

Introduction

Ab initio molecular orbital calculations on molecules comprising only hydrogen and first-row atoms occupy a voluminous portion of the present-day chemical literature. Numerous also are applications of the theory to systems incorporating second-row elements. Far less attention has been given to molecules containing third-row atoms and even less so to compounds with still heavier elements. Most ab initio calculations on molecules incorporating fourth-row or higher elements have dealt only with diatomic or triatomic species. Straub and McLean[1] employed a minimal Slater basis set supplemented by polarization functions to determine the equilibrium bond distances in HI, IF, ICl, IBr, and I_2. The theoretical quantities were found to be in close agreement with their respective experimental values. Double-ζ-type basis sets have been used in calculations on rubidium fluoride,[2a,c] strontium oxide,[2b] and rubidium oxide.[3] Here, experimental geometries were assumed. An even more extensive calculation on RbF was performed by Matcha,[4] again assuming the experimental equilibrium geometry. Here a double-ζ-type basis set was augmented by p-, d-, and f-type functions on rubidium and d- and f-type orbitals on fluorine. Bagus, Liu, Liskow, and Schaefer[5] have reported a dissociation energy and equilibrium geometry for the hypervalent XeF_2 molecule, obtained with the use of a double-ζ-type Slater basis set, supplemented by polarization functions and various levels of configuration interaction. All levels of theory employed yielded equilibrium bond lengths in good agreement with the experimental value. The XeF bond dissociation energy was not, however, found to be well reproduced unless fairly high levels of configuration interaction were introduced. Earlier calculations by these same authors on the XeF molecule[6] indicated that this species probably was not significantly bound in the gas phase. Basch, Moskowitz, Hollister, and Hankin[7] have carried out single calculations (using experimental geometries) on XeF_2, XeF_4, and XeF_6 using a Gaussian basis set of split-valence type. The properties of these hypervalent species have been discussed in terms of their results.

Several publications have appeared in which minimal Slater-type or equivalent Gaussian basis sets have been employed for calculations on molecules containing fourth-row elements. Ungemach and Schaefer[8] obtained an equilibrium bond distance of 1.61 Å for HI using a multiconfigurational SCF procedure, in excellent agreement with the experimental value of 1.609 Å. An equilibrium bond of 1.56 Å was determined by Kubach and Sidis[9] for the XeH^+ molecule. Rode[10] has performed single calculations on HI and IF molecules, as well as on the hypervalent species, IF_3, IF_5, IO_2F, IOF_3, and IO_2F_3 and their associated anions and cations. His work employed a very small Gaussian-type basis set and utilized experimental

†University of California.
‡Carnegie-Mellon University.

(1) P. A. Straub and A. D. McLean, *Theor. Chim. Acta*, **32**, 227 (1974).
(2) (a) A. D. McLean and M. Yoshimine, *IBM J. Res. Dev.*, **12**, 206 (1968); (b) *Int. J. Quantum Chem. Phys.*, 313 (1967); (c) I. Cohen, *J. Chem. Phys.* **57**, 5075 (1972).
(3) S. P. So and W. G. Richards, *Chem. Phys. Lett.*, **32**, 227 (1975).
(4) R. L. Matcha, *J. Chem. Phys.*, **53**, 4490 (1970).
(5) P. S. Bagus, B. Lin, D. H. Liskow, and H. F. Schaefer, III, *J. Am. Chem. Soc.*, **97**, 7216 (1975).
(6) D. H. Liskow, H. F. Schaefer, III, P. S. Bagus, and B. Lin, *J. Am. Chem. Soc.*, **95**, 4056 (1973).
(7) H. Basch, J. W. Moskowitz, C. Hollister, and D. Hankin, *J. Chem. Phys.*, **55**, 1922 (1971).
(8) S. R. Ungemach and H. F. Schaefer, III, *J. Mol. Spectrosc.*, **66**, 99 (1977).
(9) (a) C. Kubach, and V. Sidis, *J. Phys. B: Atom Molec. Phys.*, **6**, L289 (1973); (b) *ibid.*, **9**, L413 (1976).
(10) (a) B. M. Rode, *Chem. Phys. Lett.*, **27**, 264 (1974); (b) B. M. Rode, *J. Chem. Soc., Faraday Trans. 2*, **71**, 481 (1975).

0020-1669/81/1320-3650$01.25/0